44TH TURBOMACHINERY & 31ST PUMP SYMPOSIA
HOUSTON, TEXAS | SEPTEMBER 14 – 17 2015
GEORGE R. BROWN CONVENTION CENTER

MEASURED EFFECTS OF LIQUID DISTRIBUTION ON COMPRESSOR PERFORMANCE DURING WET GAS INGESTION

Grant O. Musgrove
Research Engineer
Southwest Research Institute
San Antonio, TX, USA

Griffin C. Beck
Research Engineer
Southwest Research Institute
San Antonio, TX, USA

Michael T. Matheidas
Group Lead - Machinery, Automation & Power
ExxonMobil Upstream Research Company
Houston, TX, USA

Stan O. Uptigrove
Machinery Lead
ExxonMobil Exploration & Production Malaysia
Malaysia

Grant O. Musgrove *is a Research Engineer in the Machinery Program at Southwest Research Institute. He currently conducts applied research for turbomachinery applications in the Oil & Gas and power generation industries. His active research areas are turbomachinery design, wet gas compression, and supercritical* CO_2.

Griffin C. Beck *is a Research Engineer in the Machinery Program at Southwest Research Institute where his responsibilities include the design, analysis, and execution of unique test programs for a wide variety of machinery, including multiphase machinery.*

Michael T. Matheidas *is currently serving as the Group Lead for the Machinery, Automation & Power group at the ExxonMobil Upstream Research Company. His industry experience has primarily been with various rotating equipment system design, start-up and troubleshooting in an assortment of global business units.*

Stan Uptigrove is the *Machinery Senior Technical Advisor for ExxonMobil Exploration and Production Malaysia Inc. Prior to this assignment; he was a Senior Machinery Engineer and Team Lead for the Machinery, Automation and Power Group at ExxonMobil Upstream Research Company.*

ABSTRACT

Upstream production of natural gas is commonly a mixture of both liquid and gas hydrocarbons that is separated before boosting the gas or liquid flows to higher pressure for transport. The gas-liquid mixture is known to affect the compressor performance, but it is not known if the distribution of the liquid entering the compressor affects the maximum amount of liquid that the compressor can safely ingest.

The work presented in this paper determines if liquid atomization affects the compressor operation or influences the amount of liquid that can be safely ingested by the compressor, compared to non-atomized liquid. To determine the effect of atomization on compressor performance, three injection methods are used to characterize the performance for atomized and non-atomized flow. Non-atomized flow is generated by injecting liquid far upstream of the compressor to allow a natural two-phase flow regime to develop before entering the compressor. Atomized flow is generated near the compressor suction flange using liquid pressure to generate large droplets on the order of 2,000 μm and gas-assisted atomization to generate droplets at least an order of magnitude less than the large droplets (100 μm). Results of the work are reported in this paper to include compressor performance measurements for two rotation speeds and a range of liquid and gas flow rates. In addition, the control of the compressor during wet gas ingestion is demonstrated through movement of the compressor on the flow map. Finally, high-speed flow images of the liquid entering the compressor are qualitatively shown to illustrate the difference in injection method.

INTRODUCTION

During typical upstream production of natural gas, the gas brought to the surface is compressed so that it can be injected into a pipeline and transported elsewhere. The gas brought to the surface is often a mixture including liquid hydrocarbons that can range in liquid content by volume from less than 1% to being the majority of the produced fluids, depending on the reservoir characteristics. Because a compressor is designed for dry gas only, the mixture of gas and liquid degrade the

performance of the compressor and historically have resulted in seal and bearing failures or even catastrophic failure of the compressor. However, most of the failures resulting from liquids are from a sudden slug of liquid entering the compressor or high velocity large droplets eroding the impellers over time. To prevent such issues and failures, the well fluids are put through a number of separation stages. These large, high pressure separation vessels can be very costly as well as adding a lot of weight and space for offshore facilities which can add significant cost to the facility. In addition, separating the gas and liquids require both pumps and compressors to boost the fluids to a high enough pressure to move them to shore or another location for processing. Furthermore, there is additional cost to having two separate pipelines or additional separation if the gas and liquids are recombined before reaching the shore or a processing facility. All of this can add significant cost and make some projects uneconomical. Therefore, there is significant cost saving potential to better understand the ability and limitations on how much liquid a centrifugal compressor can handle as well as how to make the compressor more efficiently handle higher levels of liquid.

Numerous studies have investigated the effects of gas-liquid mixtures entering centrifugal compressors to determine the effect of the liquid on compressor performance and rotordynamics [1–6,5,7,8], but were generally for liquid amounts below 5% LVF_{actual}. Very little work, however, has investigated the sensitivity of the compressor operation to the distribution of liquid entering the compressor. Brenne et al. [1] measured the effect of injecting liquid as droplets or as a film along the upstream pipe wall. The liquid was injected three pipe diameters upstream of the compressor and there was no measured effect on compressor head or flow for either form of injection. Dynamic pressure measurements recorded at the compressor inlet and discharge also did not show any difference between the liquid injection methods. The authors noted, however, that the compressor inlet may have mixed the gas-liquid such that the injection method was negligible. Fabrizzi et al. [4] measured centrifugal compressor performance while injecting liquid as both non-atomized and atomized flow. While injecting liquid at least six pipe diameters upstream of the compressor inlet, there was no significant difference between 50μm and 75μm droplet sizes. When injected directly at the compressor inlet, however, the smaller droplets were found to have less effect on compressor pressure ratio for similar liquid amounts by mass fraction (LMF). When injected upstream of the compressor inlet, the non-atomized liquid resulted in the compressor wet speed line rotating about a point at lower flow coefficient than the atomized injections. Therefore, the non-atomized liquid resulted in less rise of compressor pressure ratio at low flow coefficients compared to atomized liquid injection. Recent wet gas testing by Bertoneri et al. [6] have considered the effect of liquid droplet size on compressor operation by including a liquid injection system 20 pipe diameters upstream of the compressor. Spiral injectors were used to atomize liquid with droplet sizes 190μm and 790μm. Measured test results are not yet reported in the literature.

While previous work has indicated that the atomization of liquid entering the compressor can influence the operation, a focused effort to study the effects among different liquid distributions has not yet been done. In addition to the effect on compressor performance, it is also of value to determine if the liquid distribution affects the flow range of the compressor. In this paper, the effect on compressor performance by non-atomized, atomized large droplets, and atomized small droplets is investigated. Comparisons between injection methods are made for compressor volume flow, pressure ratio, and efficiency. The movement of the dry compressor operating point is compared between all three liquid injection methods. To observe the difference in injection method, images are recorded of liquid entering the compressor suction flange.

DESCRIPTION OF TEST LOOP

A model of the major components in the test loop is shown in Figure 1 and a Process and Instrumentation Diagram (P&ID) of the test loop is shown in Figure 2. The air loop is shown in white piping in Figure 1 as a closed-loop of 6 inch schedule 40 piping. The primary components in the air loop are the compressor, motor, gearbox, large separator, and air cooler. The air flow in the loop is controlled with a 6 inch Vee-Ball actuated valve to control the loop resistance. Opening the valve decreases the loop resistance to increase the volume flow through the compressor while closing the valve increases the loop resistance to decrease the volume flow through the compressor.

The compressor is a 1M4-2 Clark Compressor (two stage) with a maximum operating speed of 14,000 RPM and a maximum allowable discharge pressure of 34.5 barg (500 psig) based on case rating. The compressor is driven by a 700 HP electric motor with maximum operating speed of 3570 RPM and maximum torque of 400 Nm (300 ft-lb_f). The motor is controlled with a VFD that can output up to 500 volts at frequencies up to 300 Hz. A gearbox is installed between the motor and compressor with a maximum input speed of 3600 RPM and rating of 900 HP. The compressor rotor is supported by two tilt pad (on-pad) bearings and the thrust bearing installed on the non-drive end is also a tilt pad bearing.

A large separator (V-1) in the loop is used to remove water from the air loop before the air returns to compressor suction. The liquid removed from the flow is drained from the separator using loop pressure to move the water to the water tank which is at atmospheric pressure. After the separator, the air is sent to a large air cooler to remove heat added by compression. The air cooler has an actuated bypass valve to allow control of the compressor suction air temperature. Because the air is being cooled after the separator, some water condensation is expected. However, the maximum amount of water that could possibly condensate is within the uncertainty of the water flow rate measurements. The loop is pressurized to 17 bara using a mobile compressor unit rated to 24 bara (350 psi) and 200 SCMH (1300 SCFM). The loop is pressurized through the shaft end seals of the compressor continuously during testing to account for minor leakages in the air loop. Before the compressed air from the mobile

compressor enters the shaft end seals, the air is dried through a small separator (V-2).

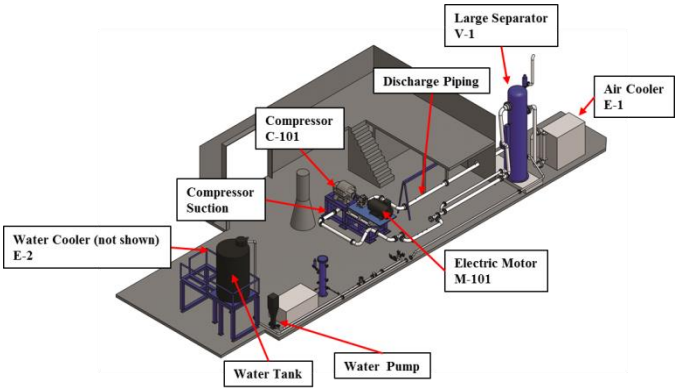

Figure 1. Solid Model Showing Major Loop Components

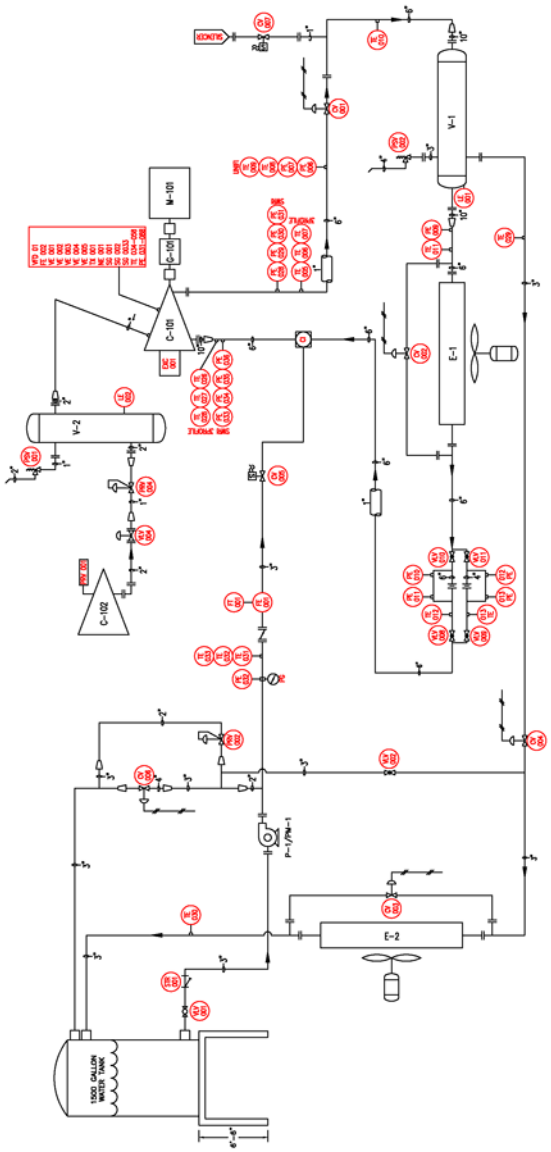

Figure 2. P&ID of the Test Loop

The water loop consists of a pump, cooler, tank, and injectors. The water pump is a 60 HP vertical unit driven by a constant speed motor. The pump has a maximum flow rate of 220 GPM and maximum working pressure of 30 bar (435 psi). Water flow is controlled using an actuated bypass valve for the pump (Vee-Ball type) and a manual globe valve for small flow rate changes. Water is provided to the pump from a 1,500 gal water tank at ambient pressure and is sent through a 3 inch Coriolis flow meter before reaching the injection manifold. From the injection manifold, water can be directed to specific water injectors in the loop. Far upstream of the compressor (44 pipe diameters), water can be directed through up to eight 10mm orifice injectors in the 6 inch air loop. Alternatively, water can be directed to injectors placed at the compressor suction flange which are varied to be seven 10mm orifice injectors or seven air-atomizing injectors. Before the water is returned to the tank, after separation, it is sent through the water cooler to remove any heat that was added during compression. Similar to the air cooler, the water cooler has an actuated bypass valve to control the water temperature returning to the tank.

MEASUREMENT AND UNCERTAINTY

The compressor loop is instrumented following ASME PTC10 guidelines in addition to other instrumentation used to monitor loop operation. In this section, only the primary measurements for compressor performance are discussed for brevity.

Air flow in the loop is measured using orifice meters placed on the suction side of the compressor. Both 4 inch and 6 inch orifice meters are used during testing to measure the full range of compressor air flow with less than ±0.1% uncertainty of the reading. Water flow is measured using a 3 inch Coriolis meter with a maximum range of 1,300 GPM and uncertainty of ±0.1% reading for flow rate greater than 50 GPM. Flow rates less than 50 GPM have a maximum uncertainty of ±0.37% reading. The uncertainties of the water and air flow measurements result in a maximum uncertainty of 0.03% LVF, absolute value. Compressor suction and discharge pressures are measured using absolute pressure transducers with a full scale range of 30 bar and uncertainty of ±0.1%FS. The maximum uncertainty of compressor pressure ratio measurements is ±0.0033. The torque meter used to measure shaft torque has a range up to 500 N-m and uncertainty of ±0.15 N-m

ATOMIZATION CONFIGURATIONS

To test the effect of droplet atomization, compressor performance is measured for small and large liquid droplets injected at the suction flange of the compressor then compared to measurements where the liquid is injected far upstream of the compressor. The different injection methods are illustrated in Figure 3 to identify the naming convention for each tested configuration.

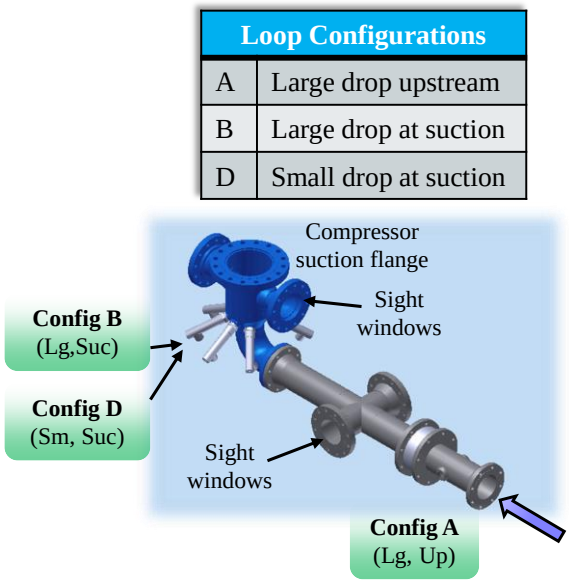

Figure 3. Naming Convention for Each Injection Configuration

In Configuration A, the liquid is injected 44 pipe diameters (22') upstream of the compressor to allow a natural two-phase flow regime to develop prior to entering the compressor. Based on a two-phase flow regime map for a 6" horizontal pipe, the flow is expected to be stratified-annular, as shown in Figure 4. The liquid is injected through up to eight orifice holes equally spaced around a 6" injection flange. Each injection port contains a 10mm diameter orifice to generate atomized droplets on the order of 2,000µm. Similar to Configuration A, Configuration B uses a 10mm diameter orifice to generate atomized droplet sizes on the order of 2,000µm near the compressor suction flange. For Configuration B, seven injectors are equally placed around the circumference of the pipe. Due to space limitation around the pipe circumference, no more than seven injectors could be used, as illustrated in Figure 5. It should be realized that the injection flange of Configuration A uses 1" injector ports with a 10mm orifice while Configuration B uses 2" injector ports with a 10mm orifice to be compatible with the interface of the small droplet nozzles near the suction flange. Small droplets of 100 µm are injected in Configuration D with an air-atomizing nozzle purchased from Spraying Systems Company. The air-atomizing nozzle uses both liquid pressure and air velocity to generate very small droplets. The 100 µm droplet size injected with Configuration D is estimated from the performance curve supplied by the manufacturer at the tested water flow rate and air differential pressure, as shown in Figure 7.

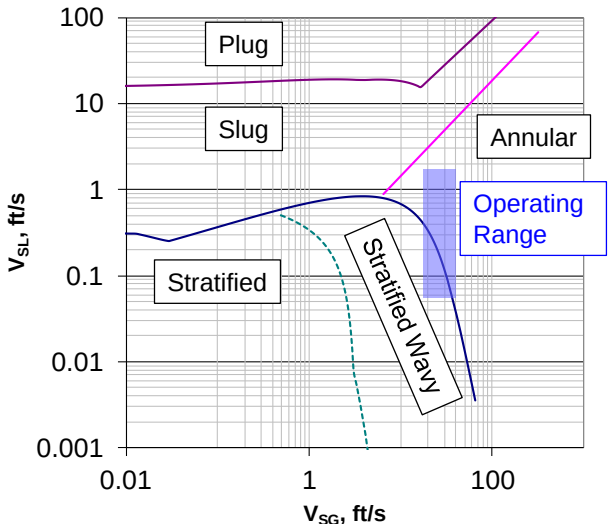

Figure 4. Estimated Flow Regime for the 6 inch Horizontal Upstream Piping to the Compressor

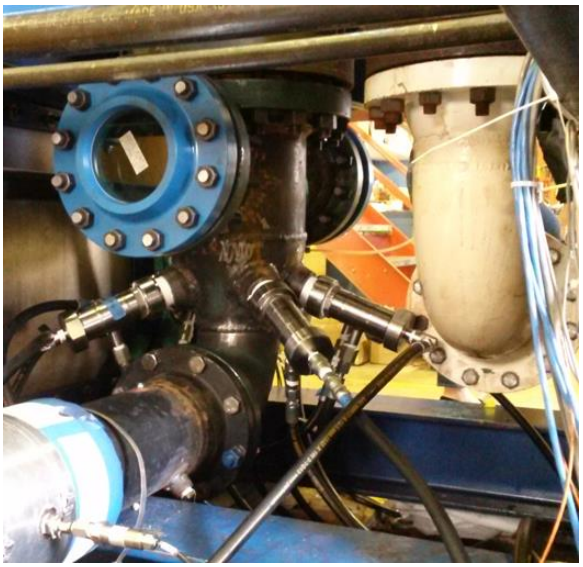

Figure 5. Installed Suction Piping with Sight Windows and Air Atomization Nozzles

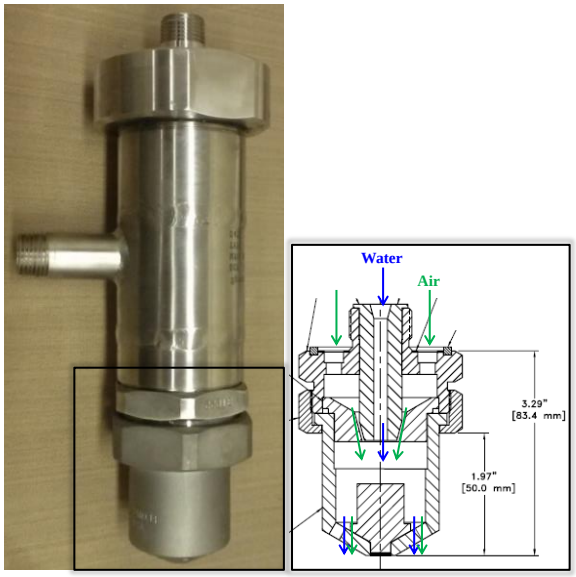

Figure 6. Small Droplet Nozzle (Configuration D)

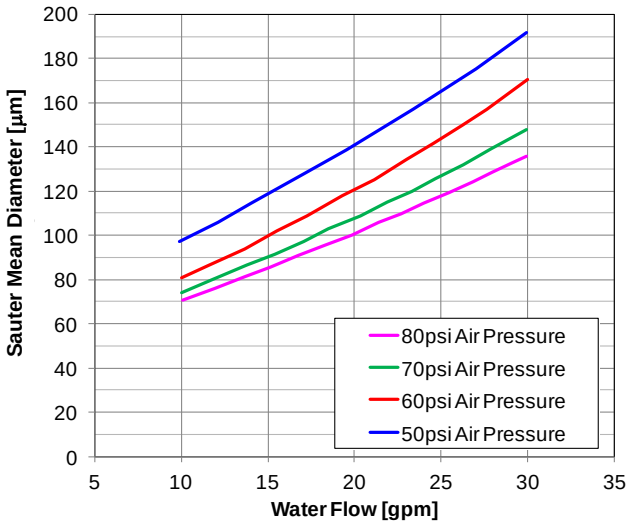

Figure 7. Nozzle Manufacturer Curves for Droplet Sizes Generated with Air-Atomizing Nozzle

TEST MATRIX

The test matrix is shown in Table 1 to include compressor speeds of 8,000 RPM and 9,500 RPM each at three air flow rates consistent with 25%, 50%, and 75% of the flow range for the speed line. For each air flow, a range of water flow rates was injected for each test configuration to measure the effect on compressor performance. The test matrix was defined with the intention of injecting nominal LVF values of approximately 1.0%, 2.8% and a maximum LVF for each compressor operating condition. Nominal LVF refers to the liquid volume fraction based on the equivalent dry air flow rate. During testing, however, it was found that the maximum LVF that could be achieved in some cases was less than 2.8%.

Table 1. Sample Test Matrix

Speed	Air Flow	Dry PR	Nominal LVF
[rpm]	[ACMH]	[-]	[-]
8,000	495 695 885	1.25 1.21 1.14	1.0%, 2.8%, *max
9,500	530 785 1025	1.37 1.31 1.21	1.0%, 2.8%, *max 1.0%, *max 1.0%, *max
* : Refer to Table 2 for max values			

Test points that were not achievable during testing were either limited by motor torque or machine vibration. Machine vibration was monitored to make sure the direct shaft vibration peak-to-peak amplitude did not exceed 0.066 mm (0.0026″). The vibration warning was set to 0.056 mm (0.0022″); however, this vibration was exceeded for some tests points to achieve maximum water flow into the compressor. Because the maximum water flow was not injected for extended periods of time (less than 1hour), exceeding the vibration warning was acceptable. The maximum direct vibration monitored during testing was 0.061mm (0.0024″). Instead of shaft vibration, motor torque was often the limiting factor for injecting the maximum amount of water into the compressor. As shaft torque reached the 400 N-m (300 ft-lb_f) motor limit during liquid injection, the speed of the induction-type motor became highly variable. To obtain steady state operation, the liquid flow rate was reduced until the motor speed was stable within ±50 RPM of the desired operating speed. The maximum measured shaft torque during testing was 390 N-m.

COMPRESSOR CONTROL DURING INJECTION

During water injection, compressor control by air flow rate was demonstrated to show that the compressor follows conventional dry-gas behavior while ingesting wet gas. For all operating conditions tested, three data points were recorded, as illustrated in Figure 8. First, dry operation was recorded without water injection. Next, compressor performance was recorded with an amount of water injected into the air flow (Mov1). Finally, the loop air flow was increased while the liquid flow rate was held constant to reduce the pressure ratio back to the dry value (Mov2), if possible. In some cases, either the liquid had negligible effect on pressure ratio (right side of the map) or the loop resistance could not be reduced enough to achieve the dry pressure ratio. It is possible that some applications may benefit from controlling speed in addition to flow due to machine vibration. However, caution must be used near the surge limit of the compressor because liquid injection reduces the compressor volumetric gas flow, as shown in Figure 8. When injecting liquid near the surge limit, the effect of the liquid on the compressor surge limit should be well understood.

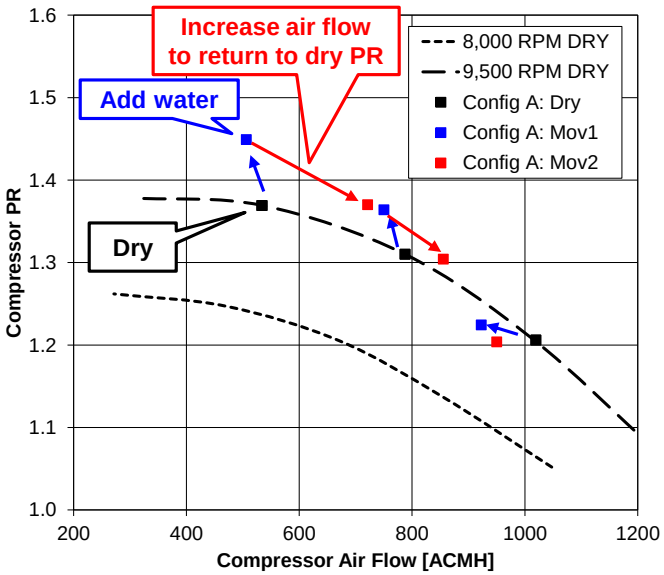

Figure 8. Air flow was used to Control Compressor Operation during Testing, Configuration A shown at 1% Nominal LVF.

COMPRESSOR PERFORMANCE MEASUREMENTS

The effect of the injection configuration on compressor performance is first shown for each configuration separately, organized by nominal LVF. Next, compressor performance is shown for each configuration as a set of compressor performance curves for each nominal LVF value tested with the configuration. Finally, compressor performance is compared among the tested configurations at similar operating conditions. Images from high-speed video are also discussed to show the visual differences seen at the compressor inlet for each injection configuration.

Compressor operation for each injection configuration

Compressor flow and pressure ratio performance for wet conditions is shown in Figure 9 through Figure 11 in comparison to the dry compressor performance curves. The effect of wet gas on the compressor performance curve using all three injection methods was typical in that there was a measurable effect on both compressor pressure ratio and flow rate. In fact, wet gas injection had more effect on compressor pressure ratio than air flow rate at low air flow operation. At high air flow operation, however, wet gas injection had less effect on compressor pressure ratio than compressor air flow rate. The resultant effect of wet gas injection on compressor operation was a clock-wise rotation of the dry performance curve about a fixed point on the dry curve, which was observed to be dependent on the amount of water being injected.

The maximum nominal LVF values for Configuration A are shown in Figure 9. Except for two operating flow rates, nominal LVF values higher than 2.8% were achieved during testing; whereby the maximum value achieved was 4.0%. At 8,000 RPM, higher water flow rate was not achievable for the low air flow rate due to machine vibration. The average direct radial vibration was 0.058 mm (0.0023″), and peaked at 0.061 mm (0.0024″). Other air flows tested at 8,000 RPM were limited to 3.7% nominal LVF by motor torque. It is important to note that the bearing lube oil temperature when testing Configuration A at low air flow was 20°C higher than the same tests for Configuration B and D. It is likely that the reduced stiffness from the low oil viscosity increased the vibration magnitude for high water flow. Oil temperature was higher for low air flow rate than other test points because data was recorded at the peak oil temperature before the bearing oil cooler was turned on for the compressor drive-end (DE) and non-drive-end (NDE) bearings. The oil cooler is an on/off fan cooler that uses ambient air to cool the oil before it is pumped to the compressor bearings. Because there is no control of the oil cooler, the cooler was not turned on until the ambient temperature reached the minimum bearing inlet temperature.

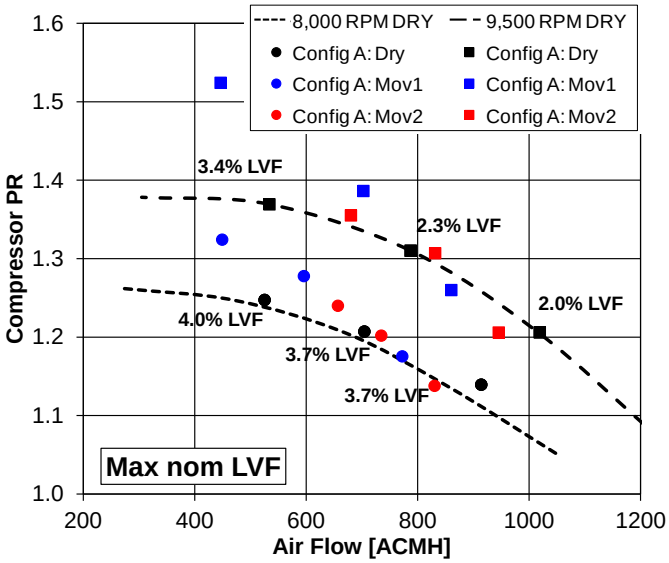

Figure 9. Compressor Operation with Configuration A (Lg, Up) for Maximum Nominal LVF

The maximum nominal LVF values that were achieved with Configuration B are shown in Figure 10. Because of the increased torque requirements when operating at 9,500 RPM, in comparison to 8,000 RPM, the maximum water flow rates for 9,500 RPM were less than 2.8% nominal LVF. The low air flow rate is shown in Figure 10 to have a maximum nominal LVF of 5.0%. However, it should be noted that up to 5.50% nominal LVF (125 GPM water) was achieved before reaching the motor torque limit. While injecting 125 GPM of water, it was found that increasing the air flow through the compressor required more torque to maintain compressor speed at 8,000 RPM. Therefore, the water flow was reduced to 113 GPM (5.0% nominal LVF) to allow the compressor operation to return to the dry pressure ratio value. For all but one test condition, motor torque was found to be the limiting factor for injecting water with Configuration B (Large, Suc). Shaft vibration limited the amount of water that could be injected for 525 ACMH nominal dry air flow at 9,500 RPM and 45 GPM water flow rate. At this condition, the bearing lube oil temperature was 10°C higher than testing the same conditions for the other two configurations such that the reduced stiffness from the low oil viscosity increased the vibration magnitude for high water flow. The high bearing oil temperature was due

to the decreased effectiveness of the oil cooler from the high ambient temperature compared to other test days.

Compressor performance with Configuration D (Sm, Suc) is shown in Figure 11 for maximum nominal LVF values. The maximum nominal LVF achieved with Configuration D was 5.4% (119 GPM) at the lowest air flow rate on the 8,000 RPM speed line. Motor torque was the limiting factor for all test conditions with Configuration D. The bearing lube oil temperature was not elevated during testing with Configuration D, as such the shaft vibration was not found to limit the amount of liquid injected that could be injection.

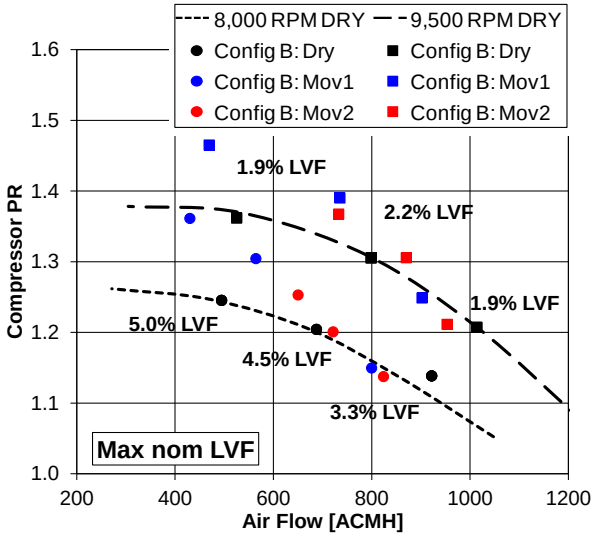

Figure 10. Compressor Operation with Configuration B (Lg, Suc) for Maximum Nominal LVF

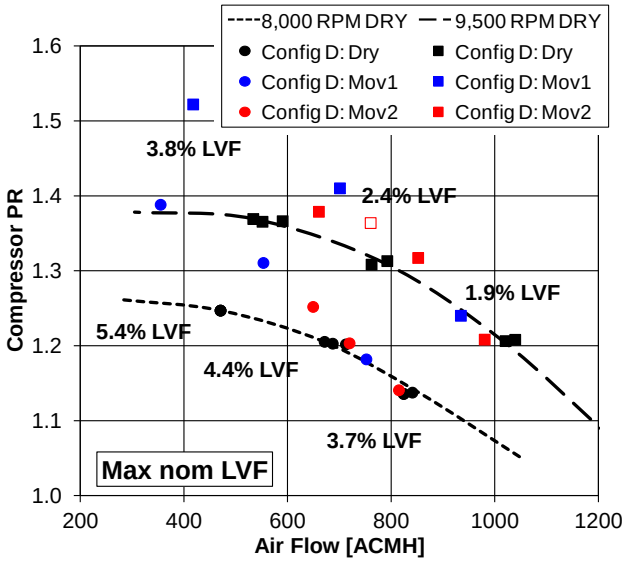

Figure 11. Compressor Operation with Configuration D (Sm, Suc) for Maximum Nominal LVF

Between the different injection methods, no correlation was found to suggest one injection method allows the compressor to ingest more water than other injection methods. In most cases, the limit on the amount of water ingestion was due to the motor torque available, while only two test points were limited by machine vibration, as summarized in Table 2. It is noted that compressor speed in-stability without reaching the motor torque limit was experienced while testing Configuration A at 695 ACMH. As mentioned earlier, the test points where machine vibration limited the amount of water that could be injected were conducted at bearing oil temperatures more than 10°C above the oil temperature for tests at the same operating point but different injection method. Configurations B and D were found to have similar maximum water ingestion, within 5 GPM, for all test points limited by motor torque.

The water ingestion limit with Configuration A, however, was found to be 20 GPM less than the limit of Configurations B and D at 690 ACMH gas flow and 15 GPM more than the limit of Configurations B and D at 920 ACMH gas flow. During testing of Configuration A at 690 ACMH gas flow, 119 GPM was the maximum amount of water that could be injected for the compressor to maintain speed ±50 RPM. Up to nearly 140 GPM was initially injected with Configuration A, but compressor speed was found to vary by as much as 400 RPM at. Because the torque limit was not reached for Configuration A at 390ACMH gas flow with 119 GPM, it is possible that the speed variation is due to liquid slugging in the vertical pipe elbow upstream of the compressor. In comparison, liquid slugging is not likely the cause for the speed variation with Configuration A for 920ACMH gas flow (155 GPM) because the motor torque limit was reached. The increased air flow velocity for 920 ACMH compared to 690 ACMH is likely the reason that liquid slugging was not occurring for the higher liquid flow with 920 ACMH gas flow.

For 920ACMH, up to 15 GPM more flow was possible with Configuration A than Configurations B and D because Configurations B and D were limited by the number of liquid injectors. While testing Configuration B and D, all injectors were open to allow the maximum water flow into the compressor. During maximum water injection, the shaft torque was measured near the maximum value to be 375 N-m and 384 N-m for Configurations B and D, but it is possible that additional water could have been added if more injectors were used. As discussed earlier, the liquid injectors for Configurations B and D were placed near the compressor suction flange and were limited to a total of 7 injectors for each configuration due to the circumferential space around the suction piping. The injectors for Configuration A, however, were located further upstream with a total of 8 injectors around the pipe circumference. More injectors were possible for Configuration A because the injector port size was smaller than Configurations B and D.

Table 2. Summary of Limiting Factors for Achieving Maximum Water Flow

Air Flow [ACMH]	Configuration A (Lg, up)		Configuration B (Lg, suc)		Configuration D (Sm, suc)	
495	*Vibration	3.9% LVF_{nom} 4.8% LVF_{act}	Motor torque	5.0% LVF_{nom} 5.7% LVF_{act}	Motor torque	5.4% LVF_{nom} 7.1% LVF_{act}
695	Compressor speed variation	3.7% LVF_{nom} 4.5% LVF_{act}	Near torque limit No.of injectors	4.5% LVF_{nom} 5.4% LVF_{act}	Near torque limit No.of injectors	4.4% LVF_{nom} 5.4% LVF_{act}
885	Motor torque	3.7% LVF_{nom} 4.5% LVF_{act}	Motor torque	3.3% LVF_{nom} 3.8% LVF_{act}	Motor torque	3.7% LVF_{nom} 4.0% LVF_{act}
530	Motor torque	3.4% LVF_{nom} 4.0% LVF_{act}	*Vibration	1.9% LVF_{nom} 2.1% LVF_{act}	Motor torque	3.8% LVF_{nom} 4.8% LVF_{act}
785	Motor torque	2.3% LVF_{nom} 2.6% LVF_{act}	Motor torque	2.2% LVF_{nom} 2.4% LVF_{act}	Motor torque	2.4% LVF_{nom} 2.6% LVF_{act}
1025	Motor torque	2.0% LVF_{nom} 2.3% LVF_{act}	Motor torque	1.9% LVF_{nom} 2.2% LVF_{act}	Motor torque	1.9% LVF_{nom} 2.2% LVF_{act}
*Vibration amplitude 2.3 mil average, 2.4 mil peak						

Comparison of Injection Methods

For direct comparison, compressor performance for all three configurations is shown in Figure 12 and Figure 13 for 1.0% and 2.8% nominal LVF, respectively. The injection configuration was found to not have a significant effect on the overall compressor performance. Specifically, the compressor wet speed curve was shown to be similar for each configuration for similar water flow rates. There was a noticeable difference, however, in the variation of compressor performance between configurations for similar test points.

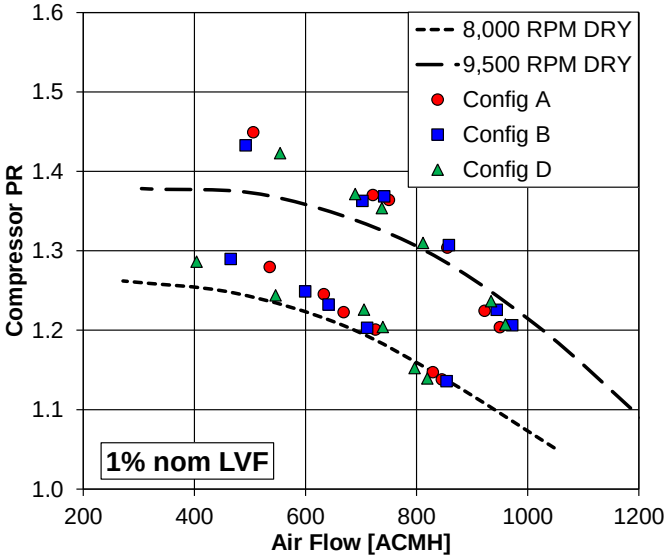

Figure 12. Compressor Performance for all configurations at 1.0% Nominal LVF

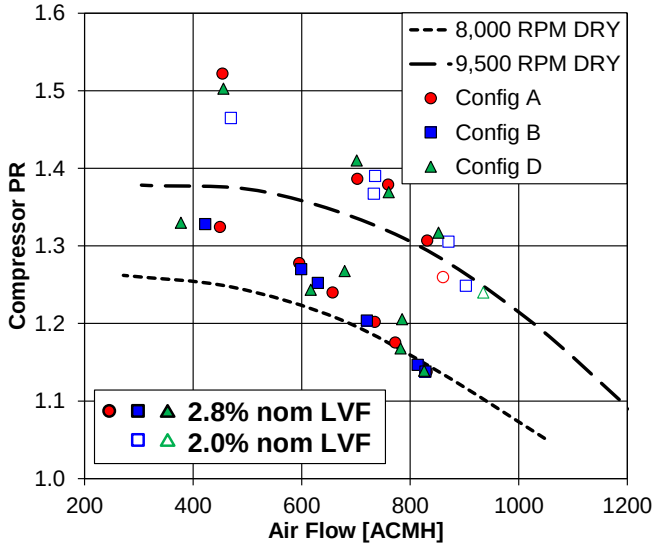

Figure 13. Compressor Performance for all Configurations at 2.8% and 2.0% Nominal LVF

To summarize, no significant effect of injection configuration on overall compressor operation was found whether liquid was ingested into the compressor suction flange as large droplets (Configuration B), small droplets (Configuration D), or a natural flow regime (Configuration A). For each injection configuration, the compressor speed line was found to remain similar to dry operation with a rotation of the speed line dependent on the amount of liquid ingested into the compressor. No discernible difference in the wet speed line was found between injection methods. The effect of injection on compressor operating range was outside the scope of this project work and was not deduced from the available measurements.

Detailed comparison of the effect of configuration on compressor operation

The compressor performance data has so far been shown in regards to general compressor operation. It was shown in

the previous section that the compressor operates along a rotated speed line that does not significantly change for different injection methods. In this section, the effect of injection method on discrete compressor operating points is shown for similar operating conditions. For direct comparison of injection configurations, only similar nominal LVF values are compared, as shown in Figure 14 and Figure 15.

For all but one of the 1.0% nominal LVF results shown in Figure 14, the compressor wet operating point moved in the same direction for all injection methods, reduced air flow and increased pressure ratio. At low air flow rate and 8,000 RPM, the compressor wet operating point with Configuration A increased in pressure ratio only while the other injection methods resulted in both lower air flow and higher pressure ratio. Some operating points showed a noticeable difference in compressor wet operation among the injection methods. For example, the compressor operating point for Configuration D moved furthest to the left on the map (reduced air flow) compared to the other two configurations at 8,000 rpm and dry air flows of 500 ACMH and 900 ACMH, as shown in Figure 14. Near 700 ACMH, however, Configuration D was seen to have negligible movement in air flow while the change in compressor pressure ratio was comparable to the other two configurations. Along the 9,500 RPM speed line in Figure 14, no significant difference between wet and dry compressor operation was seen for the injection configurations. It is important to note, however, that the scatter in operating points near 500 ACMH nominal dry flow rate 9,500 RPM is due to the scatter of the dry operating condition and not due to differing compressor responses among the injection configurations.

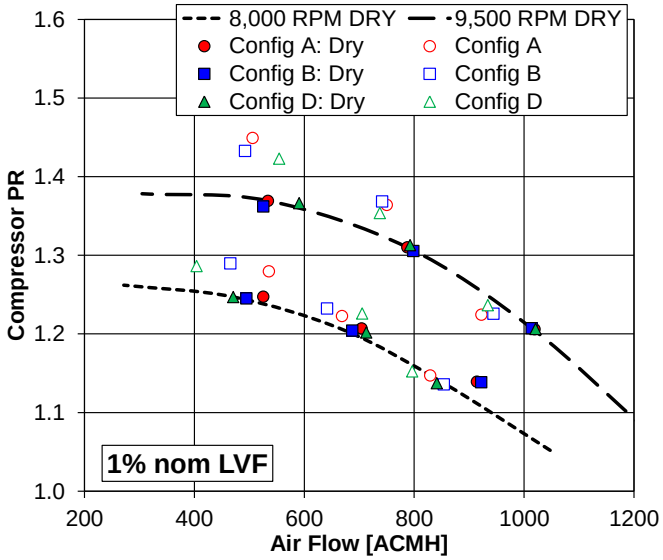

Figure 14. Change in Compressor Performance Compared Between Injection Configurations for 1.0% Nominal LVF

Similar to Figure 14, the compressor operation with water flow rates of 2.8% LVF and 2.0% LVF showed that the differences among injection configurations was typically greatest at low air flow rate. At high air flow, however, Configuration B resulted in wet compressor operation different from the other at 8,000 RPM. Specifically, Configuration B showed a reduction in air flow only while the other configurations resulted in the typical trend of reduced air flow and increased pressure ratio. The reaction of the compressor to water injection with Configuration B at this operating point was confirmed by directly switching the injection method to Configuration A without changing compressor operation or water flow rate. The resulting compressor operation with Configuration A was consistent with the measurement of Configuration D.

The water injection method was not found to affect the wet gas operating curve of the compressor. In fact, the injection method was not found to consistently affect the bulk movement of compressor operating point in relation to the dry operating point. The discrete movement of the operating point, however, was found to have significant scatter among the different injection methods. The scatter due to the injection method may suggest that there is an unobserved factor affecting the compressor performance that is not known at this time

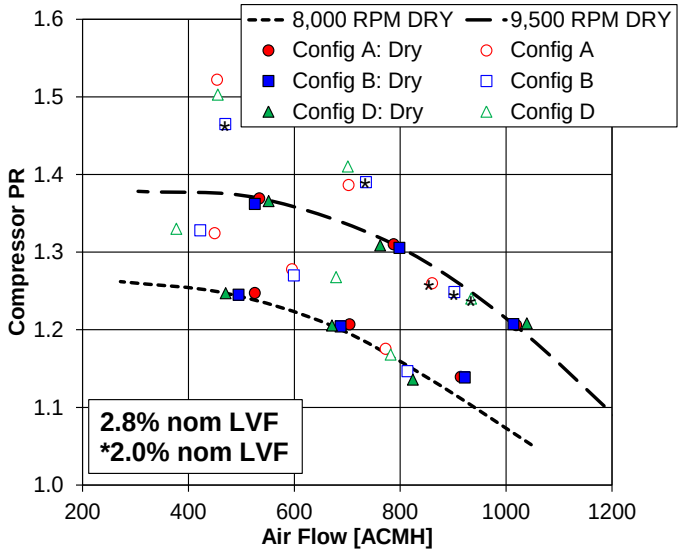

Figure 15. Change in Compressor Performance Compared Between Injection Configurations for 2.0% and 2.8% Nominal LVF

Detailed comparison of the effect of configuration on compressor power and efficiency

Similar to the compressor operation measured for different configurations, the shaft power was not found to be significantly affected by injection method, as shown in Figure 16. In fact, the compressor speed and liquid mass fraction (LMF) had a larger effect on shaft power than the injection method. The curves in Figure 16 show exponential curve fits to the 8,000 RPM and 9,500 RPM test data for all configurations in comparison to a correlation of shaft power for wet gas presented in the literature [9].

To compare the effect of the injection method on compressor efficiency, the isentropic efficiency is calculated from the shaft power and pressure ratio, as defined below. In calculating the efficiency, only the air mass flow through the compressor is considered because the volume of the liquid remains unchanged as it moves through the compressor. In other words, the liquid component does not follow a

polytropic process. Therefore, the presence of the liquid is being treated as a source of parasitic loss rather than having a direct effect on the bulk air properties through the compression process. Furthermore, isentropic efficiency is chosen for comparison instead of polytropic efficiency because of the assumptions required to calculate polytropic efficiency. Namely, the ratio of specific heats would require a bulk air-water estimate and the measured temperature ratio would assume that the air and water are at the same temperature.

$$\eta_{is} = \frac{Ideal\ Power}{Shaft\ Power} = \frac{\dot{m}_{air} C_{p,air} T_{suc} \left(PR^{(\gamma-1)/\gamma} - 1\right)}{Torque \times Speed}$$

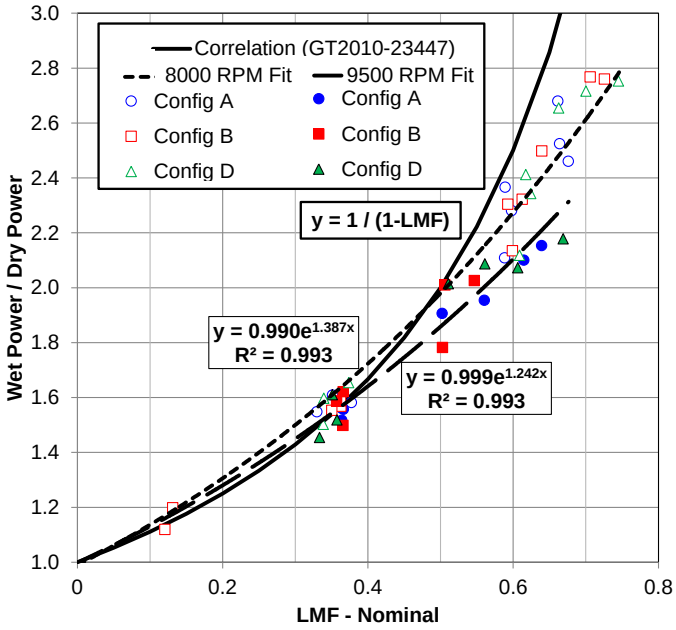

Figure 16. Effect of Configuration on Shaft Power

It was shown previously that compressor shaft power requirement increases with increasing liquid mass fraction (LMF). The increasing power requirement is likely due to a combination of increased mass flow and increased parasitic losses from the liquid. Essentially, water has a greater effect on compressor torque requirement than pressure ratio, as shown in Figure 17. The isentropic efficiency of the compressor is shown in Figure 18 to decrease as LMF is increased for both 8,000 RPM and 9,500 RPM. When comparing liquid amount among the different injection methods, the liquid mass fraction and air flow rate had much more effect on efficiency than injection method; whereby the air flow rate caused the vertical scatter in Figure 18. The effect of injection method, however, was seen when comparing discrete compressor operating points, as shown in Figure 19 for 8,000 RPM and Figure 20 for 9,500 RPM. For both compressor speeds, the range of compressor efficiency between each injection method was generally consistent as water was added. However, the greatest difference in compressor efficiency was found for low air flow rates at both 8,000 RPM and 9,500 RPM.

To further illustrate the effect on isentropic efficiency, the configurations were compared to dry performance for a single nominal LVF value of 1.0% in Figure 21 to show that the largest effect on efficiency is most visible at low air flow. At high air flow rates, less difference on efficiency was seen between the configurations. Furthermore, compressor speed was found to shift the compressor efficiency curve for wet gas compression, similar to the shift of the efficiency curve for dry gas compression.

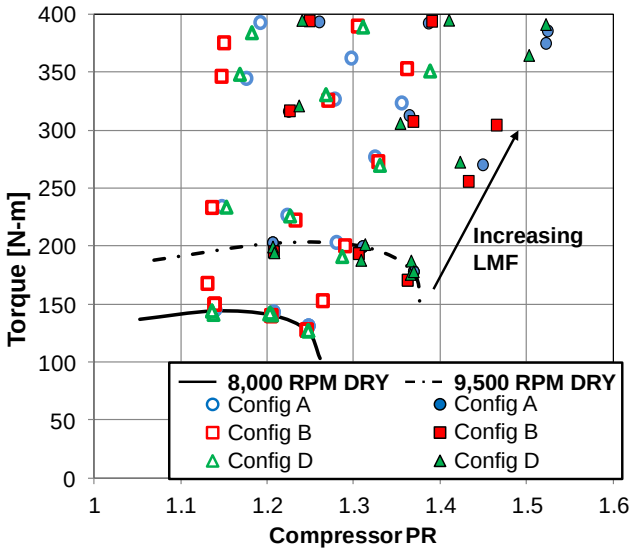

Figure 17. Water in the Compressor Affects the Torque Requirement much more than the Resulting Pressure Ratio

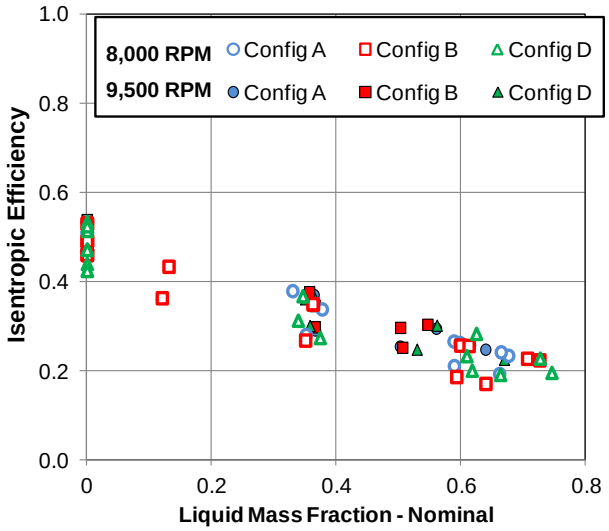

Figure 18. Effect of Injection Configuration on Isentropic Efficiency, 8,000 RPM and 9,500 RPM

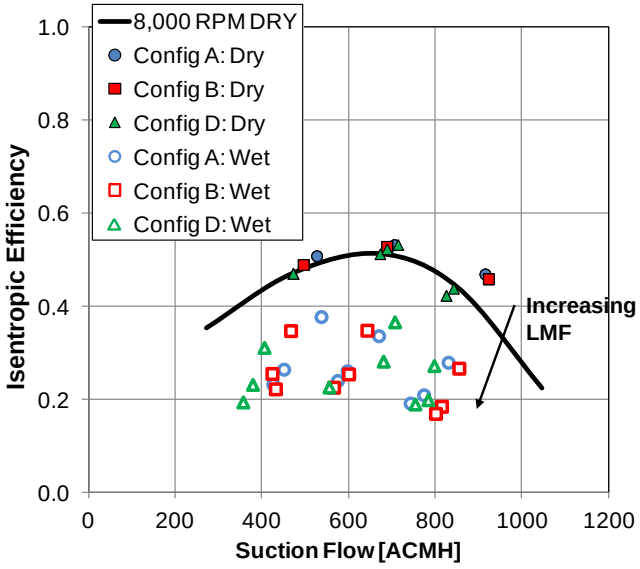

Figure 19. Effect of Injection Method on Discrete Operating Points at 8,000 RPM

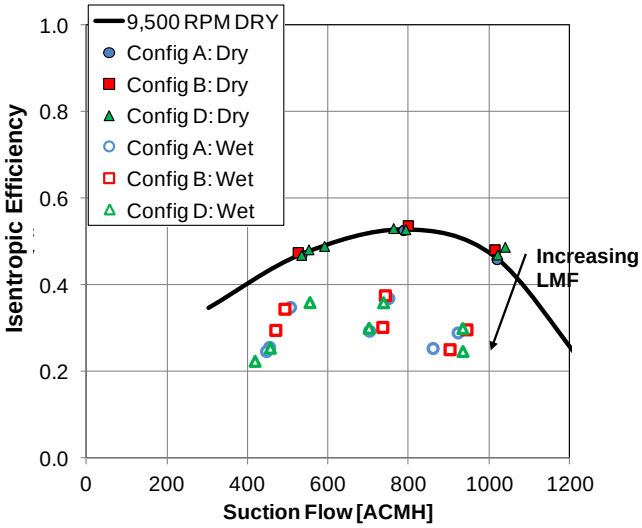

Figure 20. Effect of Injection Method on Discrete Operating Points at 9,500 RPM

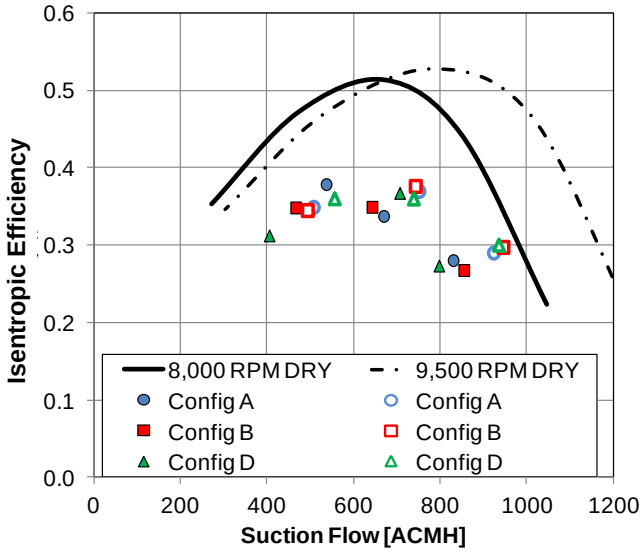

Figure 21. Effect of Configuration on Isentropic Efficiency for 1.0% Nominal LVF

IMAGES OF LIQUID FLOW ENTERING THE COMPRESSOR

Each injection method was captured using a high-speed camera placed at the sight windows near the compressor suction flange. The sight windows were placed 180° apart such that a high-intensity light was placed on the opposite side of the compressor inlet piping from the high-speed camera. Using the light opposite the camera, a shadowgraph technique was used to discern liquid flow from the gas flow. From the actual liquid flow distribution entering the compressor, no distinct small droplets could be seen. Instead, only large agglomerations were visible. High-speed video were recorded for many of the test conditions; however, selected screenshots from a handful of test conditions are presented in Table 3 to show the difference in liquid flow distribution that entered the compressor. Each image is enlarged in Figure 22 through Figure 24; whereby little difference was seen in the visible liquid distribution between Configuration A and Configuration B; whereby Configuration B showed slightly more visible liquid in the images. In contrast, Configuration D allowed the best visibility of the liquid entering the compressor. Comparing the different injection methods, it was observed that increasing the atomization of the liquid into small droplets improved visibility of the liquid. Visibility improved by the increased distance between droplets or agglomeration as the atomization level increased. Visibility of the liquid was also found to decrease as more liquid was injected into the compressor, likely because the distance between liquid agglomerations decreased with increasing liquid. Because Configuration D allowed the best visualization of the liquid, higher liquid amounts could be best seen for Configuration D only.

Table 3. Screenshots from Selected High Speed Video Showing Liquid Distribution Entering the Compressor

Operation Conditions	Configuration A (Lg, Up)	Configuration B (Lg, Suc)	Configuration D (Sm, Suc)
Q_{air} = 525 ACMH Q_{H2O} = 24 GPM LVF_{nom} = 1.10%	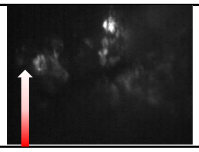	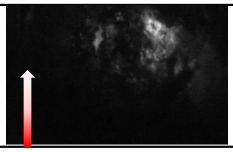	
Q_{air} = 525 ACMH Q_{H2O} = 64 GPM LVF_{nom} = 2.80%	Flow Not Visible	Flow Not Visible	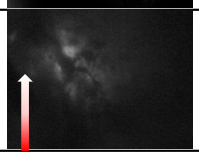
Q_{air} = 525 ACMH Q_{H2O} = 125 GPM LVF_{nom} = 5.00%	Flow Not Visible	Flow Not Visible	Flow Not Visible
Q_{air} = 915 ACMH Q_{H2O} = 42 GPM LVF_{nom} = 1.05%	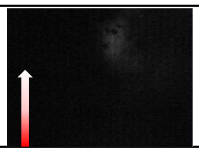	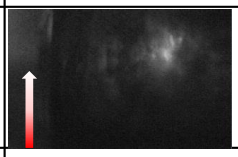	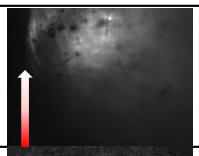
Q_{air} = 915 ACMH Q_{H2O} = 140 GPM LVF_{nom} = 3.70%	Flow Not Visible	Flow Not Visible	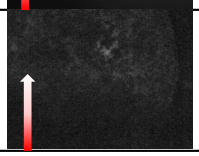

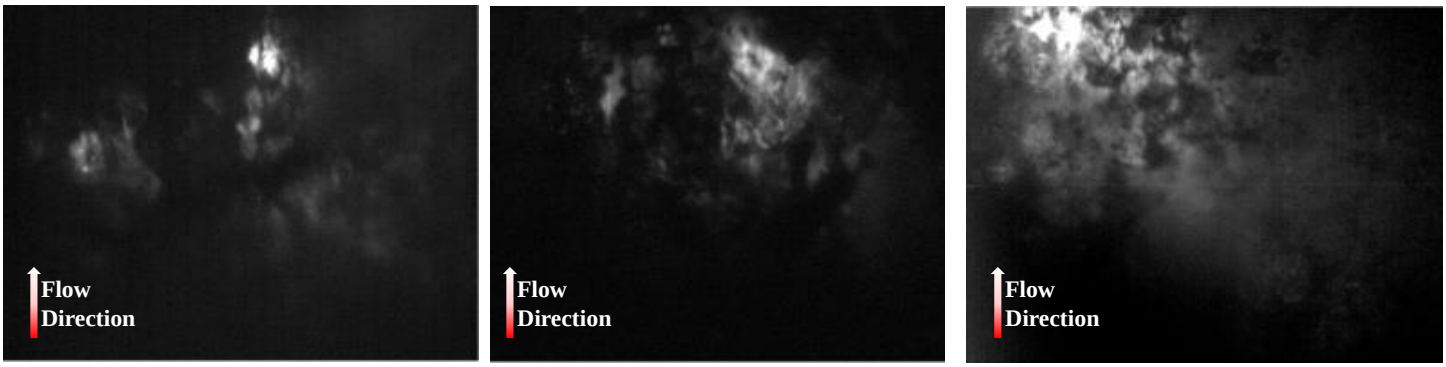

Figure 22. Air-Water Flow Entering the Compressor – 24 GPM (LVF_{nom}=1.1%); (Left) Configuration A (Lg, Up), (Middle) Configuration B (Lg, suc), (Right) Configuration D (Sm, suc).

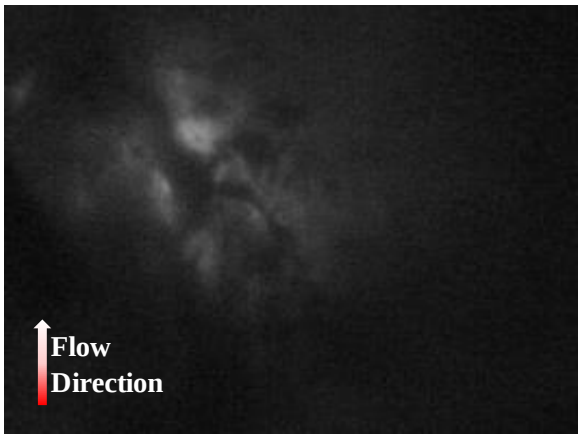

Figure 23. Air-Water Flow Entering the Compressor – 64 GPM (LVF_{nom}=2.8%); Configuration D (Sm, Suc)

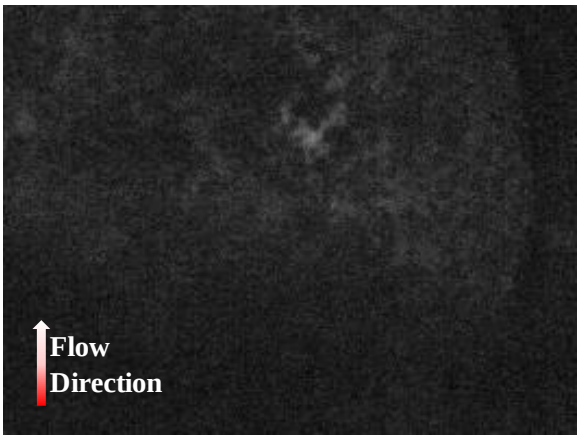

Figure 24. Air-Water Flow Entering the Compressor – 140 GPM (LVF_{nom}=3.7%); Configuration D (Sm, Suc)

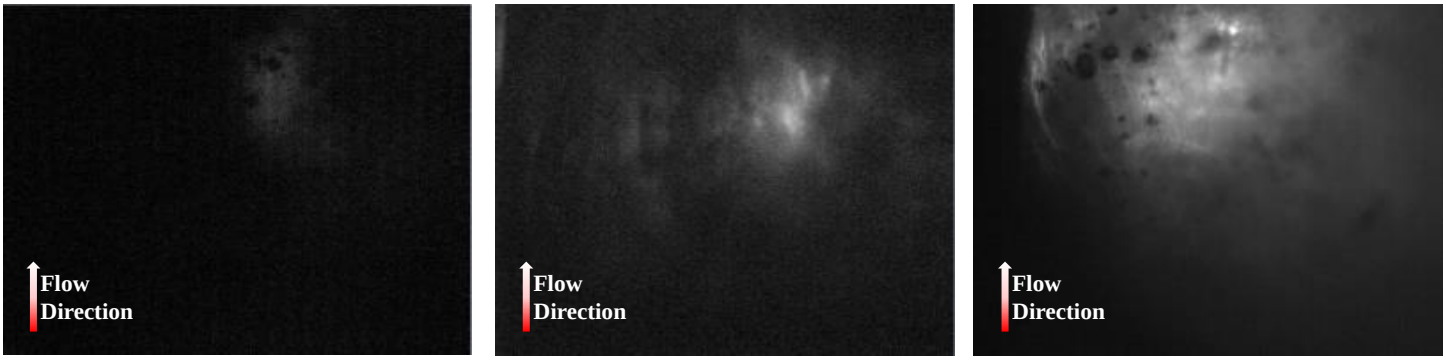

Figure 25. Air-Water Flow Entering the Compressor – 42 GPM (LVF_{nom}=1.05%); (Left) Configuration A (Lg, Up), (Middle) Configuration B (Lg, suc), (Right) Configuration D (Sm, suc).

SUMMARY AND CONCLUSIONS

In summary, the effect of atomization on compressor performance was quantified by injecting both atomized and non-atomized flow into the compressor suction flange. Both large (2000 μm) and small (100 μm) droplets were injected to measure compressor performance for a change in the order of magnitude of droplet size. Overall, it was found that the compressor operation was not significantly affected by the liquid injection method. The effect of the injection method, however, was seen for specific test points where some methods had larger effects than others on the movement of compressor operation on the performance map. The difference in operating point movement between injection methods suggested that there may be an unobserved variable affecting compressor operation. Additionally, the range of the compressor map may have been affected by injection method to possibly stretch or shrink the volume flow range of the compressor by moving the surge line to the left or right on the map. Further testing would be required to quantify the effect of wet gas on the compressor surge limit. For example, the high air flow case at 8,000 RPM was found to be of interest because the compressor operating point moved consistently to the same region after water injection with configurations A and D only. At this time it is unknown why Configuration B resulted in a different movement of the compressor operating point compared to other injection methods.

In agreement with other wet gas test results in the literature and experience at SwRI, the compressor speed line was observed to rotate as liquid amount increased. Because operating conditions nearest the curve rotation point experienced the smallest change in compressor performance, it may be useful to operate a compressor near the speed line rotation point when ingesting wet gas to have the least effect on performance.

No significant effect of injection method on compressor power requirement and efficiency was found during testing. Typical of wet gas compression, compressor power requirement increased with liquid flow while the compressor efficiency decreased. The effect of injection method did not have a greater effect than variables of liquid amount, speed, and air flow. The liquid entering the compressor was recorded using high-speed photography with a shadowgraph technique. Typically, no discernible droplets were recorded at the compressor inlet because the shadowgraph technique effectively smeared the resolution of the droplets to include liquid out of the focal plane. Unexpectedly, droplets were difficult to see at flow rates less than 40 GPM. For liquid flows of 40 GPM or higher, very little light could be seen through the flow of water entering the compressor. In fact, the small droplet atomization injection allowed the highest liquid flow rates to be recorded due to the increased distance between droplets compared to large droplet injection.

In general, the results showed that the liquid injection method had little effect on the operation of the compressor. While the liquid was atomized at the suction flange in this work, the liquid still passed through the compressor inlet scroll and inlet guide vanes before entering the impeller. It is possible that the atomized flow combined to form large droplets and ligaments before entering the compressor impeller. Future work investigating liquid atomization could inject liquid directly at the compressor impeller.

This work further demonstrates that centrifugal compressors are able to handle some liquids without damage or degradation. However, a method to control the flow of liquid to prevent slugging is still a key factor that needs further research in designing machines to be able to handle higher LMF and LVF. The effects of the liquids on the seal integrity or methods to protect the seals from liquid ingress also need to be taken into account in the design. Another option is to eliminate the seals through the use of hermetically sealed compressors.

NOMENCLATURE

Actual	Based on actual operating flow rate
ACMH	Actual cubic meters per hour
AVG	Average
GPM	Gallons per minute
LVF	Liquid Volume Fraction, $LVF = Q_l / (Q_g + Q_l)$
LMF	Liquid Mass Fraction, $LMF = w_l / (w_g + w_l)$
mil	One-thousandth of an inch (0.001 inches)
Nominal	Based on dry operating flow rate
Q	Volume flow rate
PR	Compressor pressure ratio
w	Mass flow rate

Subscripts

g	gas
l	liquid
nom	Nominal LVF
act	Actual LVF

ACKNOWLEDGMENTS

The authors wish to thank ExxonMobil Upstream Research Company for sponsoring this work and the contributions of Brandon Cassimere, Melissa Poerner, and John Stubbs.

REFERENCES

[1] Brenne, L., Bjorge, T., Gilarranz, J., and Koch, J., 2005, "Performance Evaluation of a Centrifugal Compressor Operating Under Wet Gas Conditions," Thirty-Fourth Turbomachinery Symposium, Houston, TX.

[2] Brenne, L., Bjorge, T., Bakken, L. E., and Hundseid, O., 2008, "Prospects for Sub Sea Wet Gas Compression," ASME Turbo Expo, Berlin, Germany.

[3] Shibata, T., Takahashi, Y., and Hatamiya, S., 2008, "Inlet Air Cooling with Overspray Applied to a Two-Stage Centrifugal Compressor," Proceedings of ASME Turbo Expo, Berlin, Germany.

[4] Fabrizzi, M., Cerretelli, C., Del Medico, F., and D'Orazio, M., 2009, "An Experimental Investigation of a Single Stage Wet Gas Centrifugal Compressor," Proceedings of ASME IGTI Turbo Expo, Orlando, FL.

[5] Bertoneri, M., Duni, S., Ransom, D., Podesta, L., Camatti, M., Bigi, M., and Wilcox, M., 2012, "Measured Performance of Two-Stage Centrifugal Compressor under Wet Gas Conditions," ASME Turbo Expo, Copenhagen, Denmark.

[6] Bertoneri, M., Wilcox, M., Toni, L., and Beck, G., 2014, "Development of Test Stand for Measuring Aerodynamic, Erosion, and Rotordynamic Performance of a Centrifugal Compressor Under Wet Gas Conditions," Proceedings of ASME IGTI Turbo Expo, Dusseldorf, Germany.

[7] Musgrove, G. O., Poerner, M. A., Cirri, M., and Bertoneri, M., 2014, "Overview of Important Considerations in Wet Gas Compression Testing and Analysis," 43rd Turbomachinery & 30th Pump Users Symposiua, Houston, TX.

[8] Vannini, G., Bertoneri, M., Del Vescovo, G., and Wilcox, M., 2014, "Centrifugal Compressor Rotordynamics in Wet Gas Conditions," 43rd Turbomachinery & 30th Pump Users Symposiua, Houston, TX.

[9] Gilarranz R., J., Kidd, H. A., Chochua, G., and Maier, W. C., 2010, "An Approach to Compact, Wet gas Compression," Proceedings of ASME Turbo Expo, Glasgow, United Kingdom.